Mitigation of Instrument-Dependent Variability in Ballistocardiogram Morphology: Case Study on Force Plate and Customized Weighing Scale

Yang Yao, Zahra Ghasemi, Md. Mobashir Hasan Shandhi, Hazar Ashouri, Lisheng Xu, Senior Member, IEEE, Ramakrishna Mukkamala, Senior Member, IEEE, Omer T. Inan, Senior Member, IEEE, Jin-Oh Hahn, Senior Member, IEEE

Abstract— The objective of this study was to investigate the measurement instrument-dependent variability in the morphology of the ballistocardiogram (BCG) waveform in human subjects and computational methods to mitigate the variability. The BCG was measured in 22 young healthy subjects using a high-performance force plate and a customized commercial weighing scale under upright standing posture. The timing and amplitude features associated with the major I, J, K waves in the BCG waveforms were extracted and quantitatively analyzed. The results indicated that (i) the I, J, K waves associated with the weighing scale BCG exhibited delay in the timings within the cardiac cycle relative to the ECG R wave as well as attenuation in the absolute amplitudes than the respective force plate counterparts, whereas (ii) the time intervals between the I, J, K waves were comparable. Then, two alternative computational methods were conceived in an attempt to mitigate the discrepancy between force-plate versus weighingscale BCG: a transfer function and an amplitude-phase correction. The results suggested that both methods effectively mitigated the discrepancy in the timings and amplitudes associated with the I, J, K waves between the force-plate and weighing-scale BCG. Hence, signal processing may serve as a viable solution to the mitigation of the instrument-induced morphological variability in the BCG, thereby facilitating the standardized analysis and interpretation of the timing and amplitude features in the BCG across wide-ranging measurement platforms.

Index Terms—Ballistocardiography, ballistocardiogram, force plate, weighing scale, instrument, cardiovascular signal analysis, cardiovascular signal processing

I. INTRODUCTION

The ballistocardiogram (BCG), defined as the movement of the body in response to the heartbeat, is gaining increasing interest for ultra-convenient cardiovascular (CV) monitoring by virtue of its close relationship to cardiac functions [1] as well as recent advances in the deployable and wearable instruments for unobtrusive measurement of the BCG. In fact, existing reports

This work was supported by the National Institutes of Health under Grant EB018818, the National Science Foundation under Grant CMMI-1431672, the National Natural Science Foundation of China under Grant 61773110, and the China Scholarship Council.

Yang Yao and Lisheng Xu are with the Sino-Dutch Biomedical and Information Engineering School, Northeastern University, Shenyang, China.

have revealed that the BCG waves (including the major I, J, and K waves [2]) are closely related to cardiac events and thus may possess clinical value [3]-[8]. In addition, a number of BCGmeasuring instruments assuming a wide variety of platforms have been proposed in the recent literature, including bed [9], [10], chair [11], [12], scale [13]–[15], and even wearables [16]. Leveraging these instruments (and often along with additional physiological measurements), many convenient and effective surrogate measures of CV parameters have been derived: heart rate [9], [10], pulse transit time (PTT) and pulse wave velocity [11], [17]–[20], arterial blood pressure (BP) [15], [18], [19], stroke volume and cardiac output [16], and cardiac contractility [21]–[23] to list a few. A more recent mechanistic modelingbased investigation conducted by us elucidated the physiological basis responsible for the genesis of the BCG: the BCG may originate from the BP gradients in the ascending and descending aorta [24], which indicates that the BCG has close relationship to the aortic BP waves. This finding, validated in part in our subsequent work [18], [19], may enable systematic and physiological interpretation of the BCG, in particular the timings and amplitudes of the waves therein (including the I, J, and K waves; Fig. 1(a)).

However, it has been well known that the morphology of the recorded BCG waveform largely depends on the measurement instrument as well as its coupling to the instrumented human subject. Previous investigations have indeed reported that the morphology of the recorded BCG waveform can be influenced by the difference in the instrumentation platform used [25] and its variabilities (e.g., recording surfaces and pickup types) [26], as well as the relative motion between the BCG instrument and the human body [27]. Hence, the BCG morphology recorded by a variety of instruments may exhibit heterogeneity, which may present practical challenges in analyzing and interpreting the BCG: the seemingly identical morphological features (i.e., the timings and amplitudes of the BCG waves) extracted from

Zahra Ghasemi and Jin-Oh Hahn are with the Department of Mechanical Engineering, University of Maryland, College Park, MD, USA (correspondence e-mail: jhahn12@umd.edu).

Md. Mobashir Hasan Shandhi, Hazar Ashouri, and Omer T. Inan are with the School of Electrical and Computer Engineering, Georgia Institute of Technology, Atlanta, GA, USA.

Ramakrishna Mukkamala is with the Department of Electrical and Computer Engineering, Michigan State University, East Lansing, MI, USA.

the BCG recorded with different instruments may not possess consistent relationship to the underlying CV parameters. Thus, it would be ideal if the BCG measured with heterogeneous instruments can be transformed into a reference BCG to enable standardized analysis and interpretation.

The objective of this study was to investigate the instrumentdependent variability in the morphology of the BCG waveform in human subjects and computational methods to mitigate the variability, using the BCG instrumented with a force plate and a weighing scale as a case study. Our prior work demonstrated that the BCG measured using a high-performance force plate exhibited meaningful association with clinically important CV parameters including PTT, pulse pressure, stroke volume and cardiac contractility [19], [22]. Hence, it was used as reference in this work to examine the morphological consistency of the BCG measured using a customized weighing scale, as well as to assess the efficacy of the computational methods to mitigate the morphological variability between the two BCG. For this purpose, the BCG was measured in 22 young healthy volunteers using a high-performance force plate and a customized commercial weighing scale under upright standing posture. The timing and amplitude features associated with the major I, J, and K waves in the two BCG waveforms were extracted and quantitatively analyzed. Then, two alternative computational methods were investigated in an attempt to mitigate the discrepancy between the force-plate versus weighing-scale BCG waveforms: a transfer function and an amplitude-phase correction.

This paper is organized as follows. Section 2 provides the details of data collection, signal pre-processing, data analysis, and computational methods to mitigate the instrument-induced morphological variability in the BCG. Section 3 presents the results, which are discussed in Section 4. Section 5 concludes the study with future work.

II. METHODS

A. Data Collection and Signal Pre-Processing

Under the approval of the Georgia Institute of Technology Institutional Review Board and written informed consent, the BCG was measured in 22 young healthy volunteers using a high-performance force plate (called the FP-BCG) as well as a customized commercial weighing scale (called the WS-BCG). The force plate (9260AA6, Kistler Instrument, NY, USA) has an ultra-wide bandwidth of >200 Hz, maximum body weight measurement capability exceeding 150 kg, and a high degree of signal resolution to allow for high-quality BCG recording. The customized weighing scale is built upon a commercial weighing scale (BC534, Tanita, Tokyo, Japan) by augmenting an analog amplifier and strain gauge circuitry [13]. The customized weighing scale was shown to have a bandwidth of 15 Hz for the maximum allowable body weight of 150 kg. Further details of these instruments and analog signal pre-conditioning can be found in a prior work [22]. It is worth mentioning that the force plate measures the force due to the BCG using the piezoelectric sensors while the customized weighing scale measures the body displacement in response to the force using the strain gauge

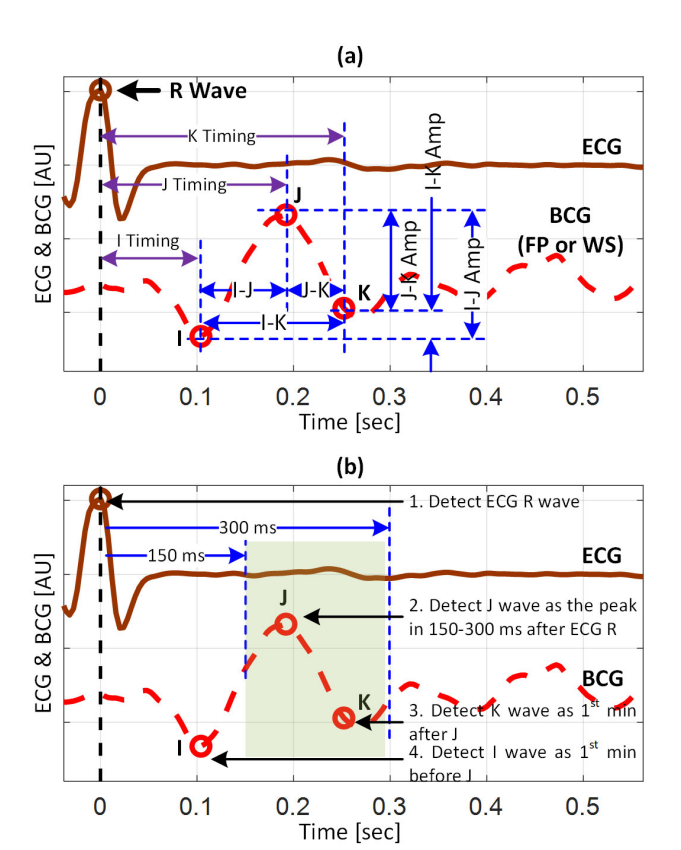


Fig. 1. Timing and amplitude features associated with the major I, J, K waves in the BCG waveform. (a) Timings, time intervals, and amplitudes. (b) BCG wave extraction procedure.

sensors. Hence, it is expected that the FP-BCG and WS-BCG are equipped with distinct waveform morphology, which needs to be mitigated to standardize the analysis and interpretation of these signals.

The subjects were asked to stand still in an upright posture for 60 seconds on the force plate as well as in the same posture for 60 seconds on the weighing scale in a randomized order. In addition to the BCG recordings, the electrocardiogram (ECG) was simultaneously measured using 3 gel electrodes in the Lead II configuration and then interfaced to a wireless amplifier (BN-RSPEC, Biopac Systems, CA, USA). Both the BCG and ECG signals were sampled at 2 kHz and then transmitted to a data acquisition equipment (MP150, Biopac Systems, CA, USA) for synchronous recording.

The acquired ECG and BCG signals were pre-processed as follows. First, the signals were zero-phase filtered with a 2nd-order Butterworth filter having the pass band of 0.5Hz – 10Hz. Second, the R wave of the ECG signal was detected as the local peak in the ECG signal. Third, the BCG signal was gated with respect to the ECG R waves to yield individual beats. Fourth, the individual BCG beats were further smoothed using a 10-beat exponential moving-average filter to suppress movement-induced artifacts [17]–[19].

B. Comparative Analysis of Force Plate and Weighing Scale BCG Waveforms

From the pre-processed BCG beats, timing and amplitude features associated with the major I, J, K waves in the FP-BCG and WS-BCG waveforms were extracted and quantitatively analyzed. Details follow.

Heart rate was computed from the R waves in the ECG as the reciprocal of the heart period (in terms of the R-R interval). In each pre-processed FP-BCG and WS-BCG beats, the J wave was identified as the local maximum between 150 ms and 300 ms after the R wave in the ECG. Then, the I and K waves were determined as the closest local minima before and after the J wave, respectively. With the I, J, and K waves thus obtained, the timings of the I, J, and K waves within the cardiac cycle relative to the ECG R wave were measured as the time interval from the ECG R wave to the I, J, and K waves, respectively, while the I-J, I-K, and J-K intervals were measured as the time intervals between the two respective BCG waves. The absolute amplitudes of the I, J, and K waves were measured as the absolute values of their heights, while the I-J, I-K, and J-K amplitudes were measured as the amplitude difference between the two respective BCG waves. To assess the quality of the extracted BCG waves, heart period computed from the BCG was compared with its ECG counterpart. Specifically, the ECG R-R interval and BCG J-J interval time series associated with each subject were compared using the paired t-test.

To assess the difference in the state of the subjects during the FP-BCG and WS-BCG measurements, the heart rate time series associated with each subject during the FP-BCG and WS-BCG recordings were compared using the unpaired t-test. quantify the limits of agreements and the significance in the differences between the timings and amplitudes of the FP-BCG versus WS-BCG, the following analysis was performed: (i) the average I, J, and K timings, I-J, I-K, and J-K intervals, I, J, and K wave amplitudes, and I-J, I-K, and J-K amplitudes associated with the FP-BCG and WS-BCG were computed in each subject; and (ii) the differences between the average I, J, and K timings, I-J, I-K, and J-K intervals, I, J, and K wave amplitudes, and I-J, I-K, and J-K amplitudes associated with the FP-BCG and WS-BCG of all subjects were examined using the mean absolute and mean absolute percent errors (MAE and MAPE), correlation analysis, Bland-Altman analysis, and the paired t-test.

C. Mitigation of Instrument-Dependent BCG Variability

Novel computational methods for mitigating the instrument-induced morphological variability in the BCG waveform were investigated by (i) constructing the representative FP-BCG and WS-BCG waveforms and (ii) developing alternative methods based on the representative BCG waveforms. Details follow.

The representative FP-BCG and WS-BCG waveforms were constructed for each subject as the average of all the gated beats. For this purpose, simple ensemble averaging and dynamic time warping techniques were considered. The representative FP-BCG and WS-BCG waveforms thus obtained were associated with different lengths due to the difference in the heart rate. To streamline the development and analysis of the computational methods by facilitating the comparison of the representative FP-BCG, WS-BCG, and FP-BCG calibrated with the computational methods, the lengths of the representative FP-BCG and WS-BCG were standardized (i.e., made identical) on the individual basis as follows: (i) the median lengths associated with all the gated FP-BCG and WS-BCG beats were calculated;

(ii) the standard BCG beat length was specified as the average of the median lengths; and (iii) the representative FP-BCG and WS-BCG waveforms were truncated to have the lengths thus specified. It is noted that the truncated small end-diastolic portion of the BCG beats may not impact the efficacy of the computational methods, because the morphology of the BCG waveform in this regime is subject to a substantial inter-subject variability that may not bear much useful information relevant to the computational methods.

The representative FP-BCG and WS-BCG beats associated with each subject thus obtained were then used to develop two alternative computational methods to mitigate the difference between the FP-BCG and WS-BCG, as outlined in detail below.

1) Transfer Function Approach

In contrast to the force plate which measures the force acting on it associated with the BCG, the weighing scale measures the displacement of the body in response to the force. Hence, the latter may be subject to an additional degree of freedom (DOF) due to the mechanical filtering of the body (as suggested by the low (<4-6 Hz) cut-off frequency associated with the mechanical impedance as well as transmissibility of vertical whole-body motions [28], [29]) not present in the former. In addition, the bandwidth of the latter is narrower than the former. Based on the simplifying assumption that these filtering effects may be lumped into a single DOF dynamics, the relationship between the FP-BCG and WS-BCG was represented by a mass-damper-spring system:

$$\mathcal{L}[y_{WS}(t)] = \frac{K_{TF}\theta_2}{s^2 + \theta_1 s + \theta_2} \mathcal{L}[y_{FP}(t)]$$
 (1)

where y_{FP} and y_{WS} denote the FP-BCG and WS-BCG, $\mathcal{L}[\cdot]$ denotes the Laplace transformation, θ_1 and θ_2 are the unknown parameters specifying the dynamic properties (i.e., bandwidth and damping ratio), and K_{TF} is the gain of the transfer function.

To utilize the representative FP-BCG and WS-BCG (which are in the form of discrete-time series sequences) in deriving the above transfer function associated with each subject, (1) was transformed into the discrete-time difference equation below by using the Euler approximation $s\cong\frac{z-1}{T_s},$ where z is the forward shift operator and T_s is the sampling time: $y_{FP}(k)=\frac{1}{K_{TF}\theta_2} \{\frac{1}{T_s^2} y_{WS}(k+2)$

$$y_{FP}(k) = \frac{1}{K_{TF}\theta_2} \left\{ \frac{1}{T_s^2} y_{WS}(k+2) + \left[\frac{\theta_1}{T_s} - \frac{2}{T_s^2} \right] y_{WS}(k+1) + \left[\frac{1}{T_s^2} - \frac{\theta_1}{T_s} + \theta_2 \right] y_{WS}(k) \right\}$$
(2)

where k is the discrete-time index. Based upon (2), the optimal transfer function parameters $\Theta^* = \{\theta_1^*, \theta_2^*, K_{TF}^*\}$ were obtained so that the root-mean-squared error (RMSE) between the actual FP-BCG time series and the FP-BCG time series derived from (2) via the pure (i.e., infinite-step-ahead) prediction [30], when inputting the measured WS-BCG time series, was minimized as follows:

$$\theta^* = \arg\min_{\theta} \left\| y_{FP}(k) - \hat{y}_{FP,TF}(k, \Theta) \right\|_{2}$$
 (3)

where $\hat{y}_{FP,TF}(k, \Theta)$ is the time series sequence of pure-predicted FP-BCG from WS-BCG via (2). The optimization problem (3)

was solved on an individual basis in order to derive subjectspecific optimal transfer functions.

2) Amplitude-Phase Correction Approach

Considering that the representative FP-BCG and WS-BCG waveforms resembled each other while the latter appeared to be phase-delayed and amplitude-attenuated relative to the former, a simple amplitude-phase correction (APC) method was conceived. The basic idea was that the WS-BCG may be obtained by applying amplitude shrinking and phase lag to the FP-BCG:

$$y_{WS}(t) = K_{APC}y_{FP}(t - T_{APC})$$
 where K_{APC} and T_{APC} are the APC parameters. (4)

The optimal correction factors K_{APC}^* and T_{APC}^* were derived on an individual basis. In each subject, K*_{APC} was derived so that the peak-to-peak amplitudes associated with the actual and APC-calibrated FP-BCG waveforms were equal:

$$K_{APC}^* = \frac{\max_{t} y_{WS}(t) - \min_{t} y_{WS}(t)}{\max_{t} y_{FP}(t) - \min_{t} y_{FP}(t)}$$
(5)
while T_{APC}^* was derived so that the J waves associated with the

actual and APC-calibrated FP-BCG waveforms were aligned:

$$T_{APC}^* = t_{WS}^J - t_{FP}^J \tag{6}$$

 $T_{APC}^* = t_{WS}^J - t_{FP}^J$ (6) where t_{FP}^J and t_{WS}^J are the time instants corresponding to the peak of the J wave associated with the FP-BCG and WS-BCG. Using K_{APC}^* and T_{APC}^* thus obtained, the FP-BCG_{APC} can be derived as follows:

$$\hat{y}_{FP,APC}(t) = \frac{1}{K_{APC}^*} y_{WS}(t + T_{APC}^*)$$
 (7)

3) Comparative Analysis of Measured and Calibrated Force Plate BCG Waveforms

To investigate the efficacy of the computational methods for mitigating the instrument-induced variability in the BCG, the limits of agreement as well as the significance in the difference between the timings and amplitudes of the actual and calibrated FP-BCG were analyzed similarly to above. Specifically, both computational methods were applied to all the individual WS-BCG beats to yield the corresponding calibrated FP-BCG beats (called the FP-BCG_{TF} and FP-BCG_{APC} beats, respectively): (i) for the transfer function approach, the WS-BCG time series of each subject was inputted to (2) characterized by the subjectspecific O* obtained from (3) to compute the FP-BCG_{TF} time series of the same subject; and (ii) for the APC approach, the WS-BCG time series of each subject was likewise inputted to (7) with the subject-specific K_{APC}^* and T_{APC}^* to compute the FP-BCG_{APC} time series of the same subject. Then, (i) the average I, J, and K timings, I-J, I-K, and J-K intervals, I, J, and K wave amplitudes, and I-J, I-K, and J-K amplitudes associated with the FP-BCG_{TF} and FP-BCG_{APC} were computed in each subject; and (ii) the differences between the average I, J, and K timings, I-J, I-K, and J-K intervals, I, J, and K wave amplitudes, and I-J, I-K, and J-K amplitudes associated with the actual FP-BCG and the calibrated FP-BCG_{TF} and FP-BCG_{APC} of all subjects were examined using the mean absolute and mean absolute percent errors (MAE and MAPE), correlation analysis, Bland-Altman analysis, and the paired t-test.

To investigate the possibility of deriving the subject-specific transfer function and APC parameters without any calibration, a simple parametric covariate analysis was performed, in which subject demographics including age, height, weight, and body

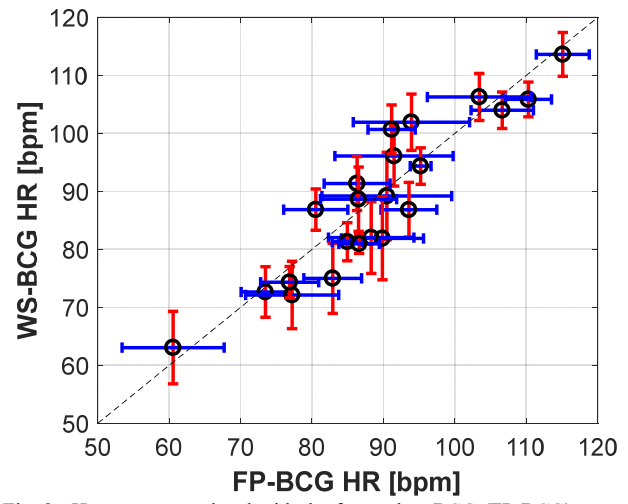


Fig. 2. Heart rate associated with the force-plate BCG (FP-BCG) versus the weighing-scale BCG (WS-BCG) recordings in all subjects (N=22). Circles and error bars indicate mean values and standard deviations, respectively.

mass index (BMI; computed as weight divided by height²) were linearly regressed to the parameters $\Theta^* = \{\theta_1^*, \theta_2^*, K_{TF}^*\}$ as well as K*APC and T*APC and the correlation coefficients between the actual and regressed parameters were examined.

III. RESULTS

Table I summarizes the demographics associated with the 22 subjects. Fig. 2 compares the heart rate of the 22 subjects associated with the FP-BCG and WS-BCG recordings. Table II shows the transfer function and APC parameters associated with all subjects. Fig. 3 compares the representative FP-BCG and WS-BCG waveforms obtained by the ensemble averaging technique. On the average, the discrepancy between the representative waveforms obtained from the ensemble averaging and dynamic time warping techniques was 3.6% for FP-BCG and 3.7% for WS-BCG in terms of RMSE relative to the RMS energy of the underlying BCG waveform. Fig. 3 also shows the Bode plots of the transfer functions along with the corresponding APC parameters (Fig. 3(b)), as well as the FP-BCG waveforms calibrated with the transfer function and APC methods (Fig. 3(a) and Fig. 3(c)). Table III summarizes the waveform RMSE and MAE between the representative FP-BCG and (i) WS-BCG as well as (ii) FP-BCG_{TF} and FP-BCG_{APC}. Fig. 4 and Fig. 5 show the Bland-Altman plots associated with the wave timings within the cardiac cycle relative to the ECG R wave and wave-to-wave intervals (Fig. 4) as well as the absolute and wave-to-wave amplitudes (Fig. 5), between the FP-BCG and (i) WS-BCG, (ii) FP-BCG_{TF}, and (iii) FP-BCG_{APC} in all subjects. Table IV shows the MAE, MAPE, and correlation coefficients between the FP-BCG and (i) WS-BCG, (ii) FP-BCG_{TF}, and (iii) FP-BCG_{APC}. Table V shows the correlation coefficients between subject demographics and transfer function as well as APC parameters.

Table I: Subject demographics (mean (SD)). FP-BCG beats and WS-BCG beats indicate the number of FP-BCG and WS-BCG beats extracted from data for analysis.

| Age | Gender | Height | Weight | FP-BCG | WS-BCG |
|-------|------------|--------|--------|--------|--------|
| [Yr] | Gender | [cm] | [Kg] | Beats | Beats |
| 25.2 | 9 Males | 170.7 | 72.2 | 110 | 111 |
| (5.7) | 13 Females | (14.0) | (24.9) | (38) | (37) |

Table II: Transfer function and amplitude-phase correction parameters associated with all subjects (mean (SD)).

| Transfer Function | | Amplitude-Phase Correction | | |
|-------------------|--------------|----------------------------|-------------|------------|
| θ_1^* | θ_2^* | K_{TF}^* | K_{APC}^* | T*APC [ms] |
| 943 | 64843 | 0.61 | 0.75 | 15 |
| (1193) | (84720) | (0.12) | (0.17) | (3) |

Table III: Sample-by-sample waveform root-mean-squared errors (RMSEs) and mean absolute errors (MAEs) between representative force-plate BCG (FP-BCG) and (i) weighing-scale BCG (WS-BCG) as well as (ii) FP-BCG calibrated with transfer function (FP-BCG $_{TF}$) and amplitude-phase correction (FP-BCG $_{APC}$) methods in all subjects (N=22) (mean (SD)). TF: Transfer function. APC: Amplitude-phase correction. *: P<0.001 WITH RESPECT TO WS-BCG (PAIRED T-TEST).

| | WS-BCG | FP-BCG _{TF} | FP-BCG _{APC} |
|----------|-------------|----------------------|-----------------------|
| RMSE [N] | 0.04 (0.02) | $0.02(0.01)^*$ | $0.02(0.01)^*$ |
| MAE [N] | 0.03 (0.01) | $0.02(0.01)^*$ | $0.02(0.01)^*$ |

IV. DISCUSSION

The BCG has attracted increasing interest for enabling ultraconvenient CV health monitoring by virtue of its amenity to unobtrusive measurement using a wide variety of instruments. However, the BCG recorded by different instruments exhibit heterogeneity in morphology, making it difficult to translate the physiological insights on the BCG and its relationship to arterial BP waves universally to heterogeneous BCG recordings, and also to generalize effective surrogate measures of CV parameters derived from the BCG recorded with one instrument to the other BCG recorded with different instruments. Hence, eliminating the instrument-dependent morphological variability in the BCG waveform can open up unprecedented opportunities for standardized analysis and interpretation of the BCG. In this study, we conducted a preliminary case study of comparing the BCG instrumented with a high-performance force plate (FP-BCG) and a commercial weighing scale (WS-BCG) to illustrate the instrument-dependent variability in the BCG morphology, and also to develop computational methods equipped with the potential to mitigate such a variability.

A. Experimental Data

From both the FP-BCG and WS-BCG recordings, an average of >100 beats could be extracted from each subject for analysis conducted in this study (Table I). The difference in the heart rate values associated with the FP-BCG and the WS-BCG were insignificant in all subjects (p>0.05; Fig. 2). Hence, it may be concluded that the physiological state of the subjects remained quite consistent during the instrumentation of the FP-BCG and WS-BCG, despite the fact that the two BCG were not recorded simultaneously.

In all subjects, the ECG R-R interval and BCG J-J interval time series were not significantly different (p>0.05) with small MAE (FP-BCG: 1.8+/-1.2 ms; WS-BCG: 1.7+/-0.8 ms), which strongly suggested the quality of the extracted BCG waves.

Table IV: Mean absolute errors (MAEs), mean absolute percent errors (MAPEs), and correlation coefficients between force-plate BCG (FP-BCG) and (i) weighing-scale BCG (WS-BCG) as well as (ii) FP-BCG calibrated with transfer function (FP-BCG_{TF}) and amplitude-phase correction (FP-BCG_{APC}) methods in all subjects (N=22). TF: Transfer function. APC: Amplitude-phase correction.

(a) Mean absolute errors (timings: [ms], amplitudes: [N])

| | WS-BCG | FP-BCG _{TF} | FP-BCG _{APC} |
|------------------|--------|----------------------|-----------------------|
| I Wave Timing | 13.76 | 1.8 | 2.58 |
| J Wave Timing | 14.95 | 1.07 | 0.37 |
| K Wave Timing | 14.5 | 3.1 | 3.29 |
| I-J Interval | 2.24 | 2.09 | 2.24 |
| I-K Interval | 3.65 | 4.01 | 3.65 |
| J-K Interval | 3.27 | 3.69 | 3.27 |
| I Wave Amplitude | 0.19 | 0.05 | 0.07 |
| J Wave Amplitude | 0.28 | 0.03 | 0.04 |
| K Wave Amplitude | 0.2 | 0.05 | 0.06 |
| I-J Amplitude | 0.46 | 0.05 | 0.07 |
| I-K Amplitude | 0.12 | 0.09 | 0.1 |
| J-K Amplitude | 0.47 | 0.05 | 0.04 |

(b) Mean absolute percent errors ([%])

| | WS-BCG | FP - BCG_{TF} | FP - BCG_{APC} |
|------------------|--------|-------------------|--------------------|
| I Wave Timing | 13 | 2 | 2 |
| J Wave Timing | 8 | 1 | 0 |
| K Wave Timing | 5 | 1 | 1 |
| I-J Interval | 3 | 2 | 3 |
| I-K Interval | 2 | 2 | 2 |
| J-K Interval | 3 | 4 | 3 |
| I Wave Amplitude | 29 | 8 | 12 |
| J Wave Amplitude | 25 | 3 | 4 |
| K Wave Amplitude | 26 | 8 | 9 |
| I-J Amplitude | 27 | 3 | 5 |
| I-K Amplitude | 96 | 82 | 100 |
| J-K Amplitude | 25 | 3 | 2 |

(c) Correlation coefficients

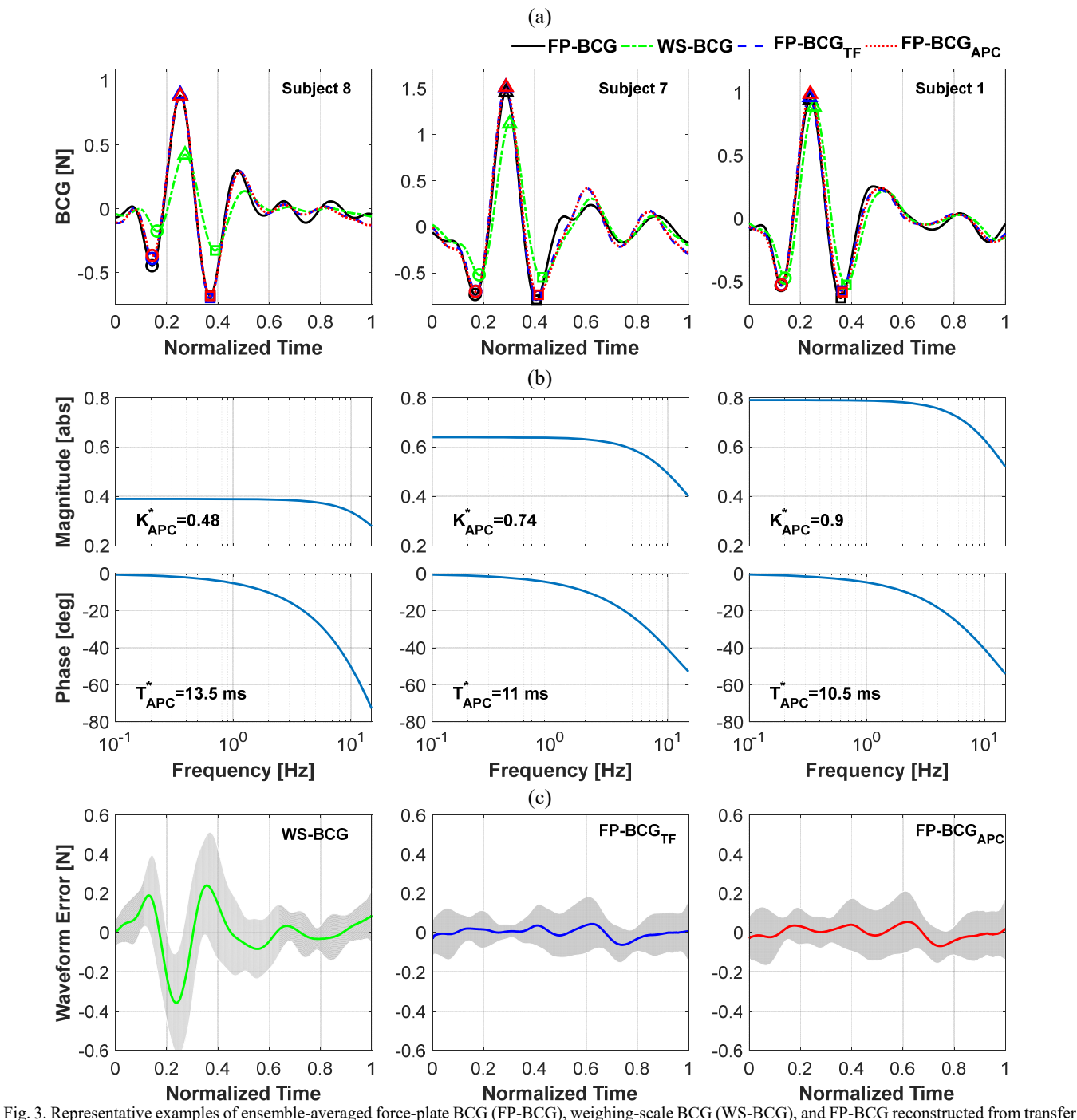
| WS-BCG | FP - BCG_{TF} | FP - BCG_{APC} |
|--------|--------------------------------------------------------------------------------------|--------------------------------------------------------------------------------------------------------------------------------------------------------------------------------------------------------------------------------------------------------------------------------------------------------|
| 0.97 | 0.99 | 0.98 |
| 0.99 | 1 | 1 |
| 0.99 | 0.98 | 0.99 |
| 0.92 | 0.95 | 0.92 |
| 0.96 | 0.93 | 0.96 |
| 0.92 | 0.88 | 0.92 |
| 0.85 | 0.96 | 0.89 |
| 0.87 | 0.99 | 0.99 |
| 0.76 | 0.97 | 0.97 |
| 0.88 | 0.99 | 0.98 |
| 0.69 | 0.83 | 0.8 |
| 0.83 | 0.99 | 1 |
| | 0.97 0.99 0.99 0.92 0.96 0.92 0.85 0.87 0.76 0.88 0.69 | 0.97 0.99 0.99 1 0.99 0.98 0.92 0.95 0.96 0.93 0.92 0.88 0.85 0.96 0.87 0.99 0.76 0.97 0.88 0.99 0.69 0.83 |

Table V: Correlation coefficients between subject demographics (including age, height, weight, and body mass index) and (i) transfer function as well as (ii) amplitude-phase correction parameters.

| Transfer Function | | Amplitude-Phase Correction | | |
|-------------------|--------------|----------------------------|-------------|------------------------|
| θ_1^* | θ_2^* | K_{TF}^* | K_{APC}^* | T* _{APC} [ms] |
| 0.58 | 0.66 | 0.26 | 0.47 | 0.45 |

B. Comparative Analysis of Force Plate and Weighing Scale BCG Waveforms

Comparing the FP-BCG and the WS-BCG, the latter showed phase lag and amplitude attenuation relative to the former (Fig. 3). On the average, the timings of the I, J, and K waves within the cardiac cycle relative to the ECG R wave were lagged by 14 ms, 15 ms, and 15 ms, respectively (as can be seen by the value of T_{APC} in Table II), relative to the FP-BCG, which amounted to 13% (I), 8% (J), and 5% (K) of the respective wave timings



function (FP-BCG_{TF}) and amplitude-phase correction (FP-BCG_{APC}) methods. (a) Representative waveforms associated with the subjects with a large (left), average (center), and small (right) morphological variability between FP-BCG and WS-BCG. Circles: I wave. Triangles: J wave. Squares: K wave. (b) Bode plots of the transfer functions and the corresponding APC parameters. (c) Mean (solid line) and standard deviation (shade) of waveform errors associated with WS-BCG, FP-BCG_{TF}, and FP-BCG_{APC} across all subjects.

relative to the ECG R wave. Moreover, the amplitudes of the waves were attenuated by 0.18 N, 0.28 N, and 0.18 N, respectively, relative to the FP-BCG, which amounted to 28% (I), 26% (J), and 22% (K) of the respective wave amplitudes (as can be seen by the values of K*_{TF} and K*_{APC} in Table II). In addition, the phase lag and amplitude attenuation were subject to substantial variability in different subjects (>20% in terms of the coefficient of variation associated with the APC parameters; Table II). In contrast to the timings and absolute amplitudes, the time intervals between the I, J, and K waves as well as the

amplitude ratios between these waves were quite comparable to the FP-BCG (Table IV). On the average, the I-J, I-K, and J-K intervals associated with the FP-BCG versus the WS-BCG were different only by 1%, 1%, and 0%, respectively, and as well, the I-J, I-K, and J-K amplitude ratios associated with the FP-BCG versus the WS-BCG were different only by 2%, 3%, and 0%, respectively. However, the difference may not be consistently negligible due to non-trivial beat-by-beat variability of the intervals (4+/-2% (I-J), 3+/-3% (I-K), and 5+/-5% (J-K) for the FP-BCG and 4+/-2% (I-J), 3+/-2% (I-K), and 5+/-4% (J-K) for

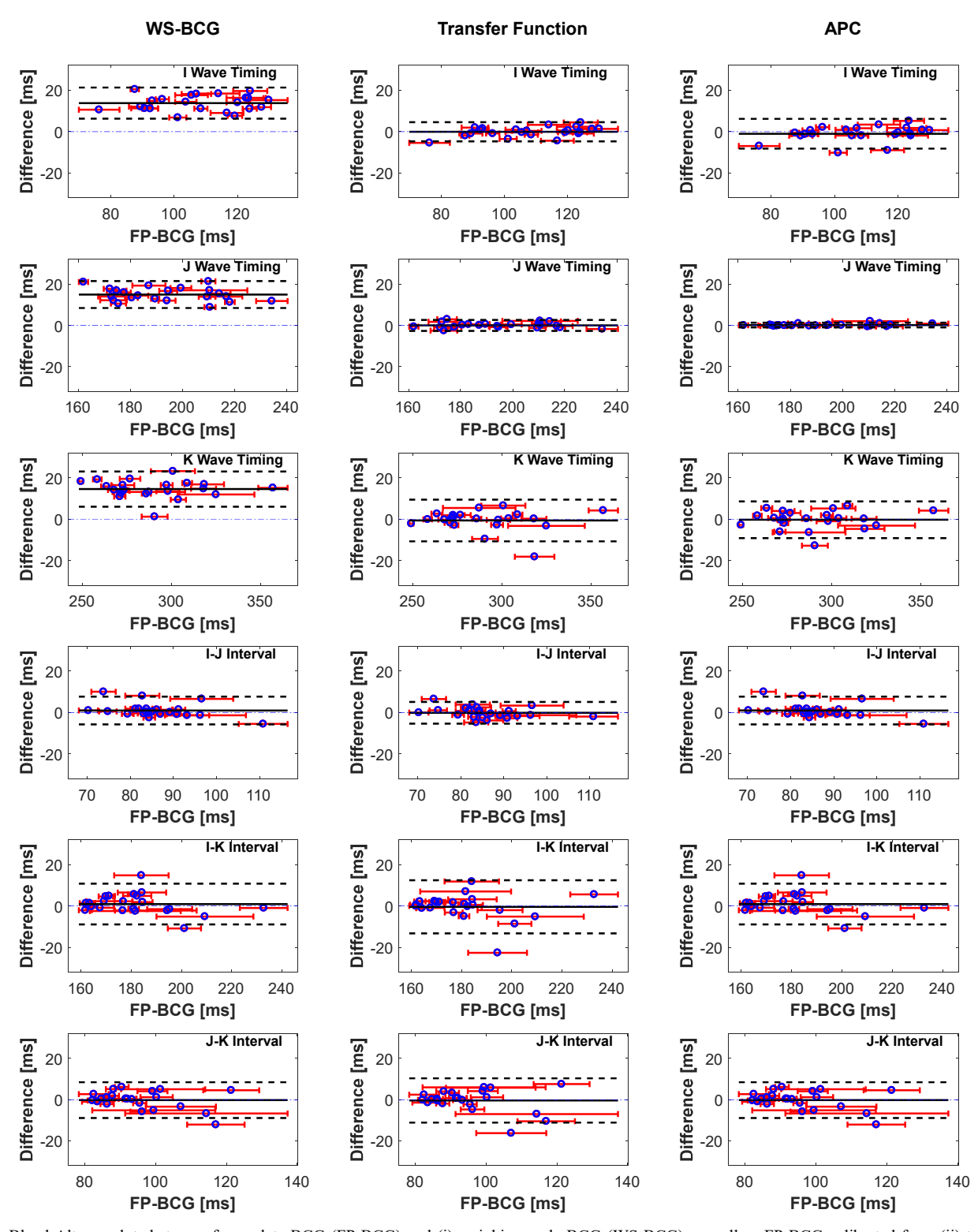


Fig. 4. Bland-Altman plots between force-plate BCG (FP-BCG) and (i) weighing-scale BCG (WS-BCG) as well as FP-BCG calibrated from (ii) transfer function and (iii) amplitude-phase correction (APC) methods in all subjects (N=22): wave timings within cardiac cycle relative to ECG R wave and wave-to-wave intervals.

the WS-BCG, all in terms of the coefficient of variation) and amplitudes (11+/-4% (I-J), 123+/-105% (I-K), and 10+/-4% (J-K) for the FP-BCG and 12+/-4% (I-J), 241+/-325% (I-K), and 11+/-5% (J-K) for the WS-BCG, all in terms of the coefficient of variation). Overall, the results clearly indicated that the FP-BCG and the WS-BCG are distinct in morphology, and that the

pattern of distortion (i.e., the phase lag and amplitude attenuation) is variable in individual subjects, although the qualitative pattern appears to remain consistent.

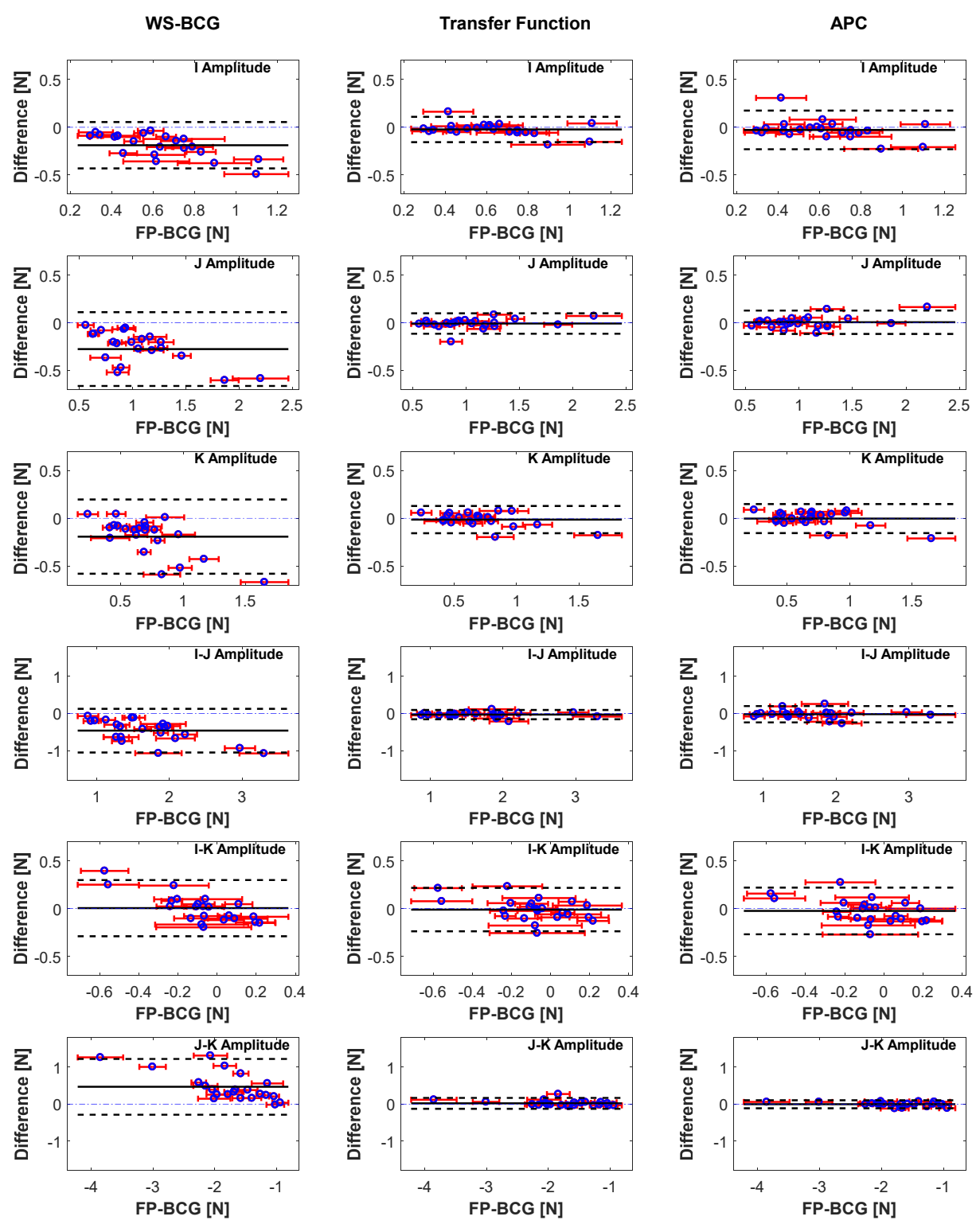


Fig. 5. Bland-Altman plots between force-plate BCG (FP-BCG) and (i) weighing-scale BCG (WS-BCG) as well as FP-BCG calibrated from (ii) transfer function and (iii) amplitude-phase correction (APC) methods in all subjects (N=22): absolute and wave-to-wave amplitudes.

The correlation analysis revealed findings consistent with the above observations associated with the absolute errors: (i) the absolute amplitudes of the I, J, and K waves (including the wave-to-wave amplitudes) exhibited relatively low r values, whereas (ii) the time intervals between the I, J, and K waves showed high r values (Table IV). One exception contrasting to the findings related to the absolute errors was that the timings

within the cardiac cycle of the I, J, and K waves relative to the ECG R wave showed high r values, which may be attributed to the large ranges of these timings compared to the phase lag between the FP BCG and the WS-BCG.

Overall, the results suggest that the large morphological discrepancy between the FP-BCG and WS-BCG may prevent the universal analysis and interpretation of the BCG signal. In

regards to the analysis, the integrity of the WS-BCG's timings, time intervals, and amplitudes can be degraded relative to the FP-BCG. For example, it is plausible that the efficacy of the PTT based on the FP-BCG [18] as well as its J-K amplitude [19] may be impaired in case they are constructed using the WS-BCG, since they may be more susceptible to the measurement resolution and noise due to shorter duration (i.e., the BCG waves, which serve as the proximal timing reference for PTT, are delayed) and smaller amplitude (i.e., the waves are attenuated). In regards to the interpretation, the physiological understanding of the WS-BCG may need to take into account the masked effect of instrument dynamics as well as mechanical filtering of the body. It is admitted that the adverse influence of the morphological discrepancy induced by the instruments may not be extreme in the case of FP-BCG and WS-BCG due to the consistency in the measurement site. However, it may present more profound challenges if combined with diversity in the measurement sites (e.g., foot, arm, wrist, and ear) and even postures (e.g., standing, sitting, and supine).

C. Mitigation of Instrument-Dependent BCG Variability

The representative FP-BCG and WS-BCG obtained from the ensemble averaging and dynamic time warping techniques were highly similar to each other, which led us to use the ensemble averaging technique in the subsequent analysis. It is speculated that simple ensemble averaging of the BCG beats may suffice for the analysis conducted in this study based on the following observations: (i) the recording was very short (approximately only 1 min long in all subjects) and the variability in the beat length was small (0.04 seconds on the average in terms of standard deviation); and (ii) the I-J-K complex in all the gated beats were quite well aligned despite the variability in the beat length.

Both computational methods developed in this study were very effective in mitigating the difference between the FP-BCG and the WS-BCG. First, the methods could largely reduce the morphological discrepancy between the two BCG by making up for the phase lag and amplitude attenuation (Fig. 3-Fig. 5). In fact, the RMSE and MAE between the FP-BCG and the FP-BCG_{TF} and the FP-BCG_{APC} were significantly smaller than those between the FP-BCG and the WS-BCG by 50% and 49% as well as 46% and 45%, respectively, on the average (Table III). In terms of the timings and amplitudes of the BCG waves, both computational methods led to the calibrated BCG with significantly improved agreement with the FP-BCG (Table IV): (i) the errors associated with the timings and amplitudes of the I, J, and K waves were smaller than those associated with the WS-BCG, while (ii) the I-J, I-K, and J-K intervals associated with the WS-BCG and both the FP-BCG_{TF} and FP-BCG_{APC} were comparable to and not significantly different from those associated with the FP-BCG. In addition, the correlation analysis also indicated that both computational methods could improve the correlation coefficients associated with the wave timings and amplitudes, thereby supporting their efficacy in mitigating the instrument-induced variability in the BCG morphology (Table IV).

The results obtained from the parametric covariate analysis showed that a subset of transfer function and APC parameters may be reasonably well correlated with the demographics of the subjects, but the absolute degree of correlation was not very high (Table V). Thus, it may be concluded that subject-specific transfer function and APC parameters may not be easily derived from rudimentary linear regression based on the demographics, and that additional predictors (e.g., properly normalized WS-BCG features) and more advanced regression techniques may be required to faithfully determine subject-specific calibration parameters for the transfer function and APC methods.

Overall, the results obtained from the computational methods suggested that signal processing may serve as a viable basis for the mitigation of instrument-induced morphological variability in the BCG waveform to facilitate the standardized analysis and interpretation of clinically meaningful features therein. But at the same time, obtaining subject-specific calibration remains an open challenge that must be addressed in the future work.

A critical challenge remains unanswered as to how to extend the findings from this study to standardize the BCG originating from diverse measurement sites, postures, and instrument types (i.e., the quantities measured by the instrument). It is expected that calibrating the BCG from the body's extremity sites (e.g., ear and wrist) to the FP-BCG may require the integration of the body's musculoskeletal dynamics into the calibration methods. For example, a lumped-parameter model dictating the vibration transfer in the body may be incorporated in developing the transfer function method. Such a model may also be useful in accommodating the variability associated with the instrument types, by virtue of its capability to compute a range of physical quantities at various body sites, e.g., the forces, displacements, velocities, and accelerations at the extremity sites in the body. Alternatively, purely data-driven approaches similar to the APC method may also be conceived. On the other hand, the effects of diverse postures, especially those related to the extremity sites, may require the use of extra sensors (e.g., gyroscope) that can inform the sites' position and orientation for the correction of the posture-induced artifacts.

D. Study Limitations

This study has a few limitations. First, the enrolled subjects were homogeneous in terms of age. In order to investigate the generalizability of the findings derived from this study, it would be of interest to examine the morphological discrepancy in the BCG as well as the efficacy of the computational methods in more diverse subjects in terms of not only age but also other factors (e.g., height and weight). It would also be of interest to expand the study to the BCG recordings obtained from diverse instruments such as arm and wrist bands as well as earphones. Second, the BCG recordings were obtained only in a resting To establish more comprehensive insights on the morphological discrepancy in the BCG and the robustness of the computational methods under diverse physiological state, future work must conduct studies involving interventions that largely alter the subject's physiological state. Third, the effect of respiration on the robustness of the findings from this study needs to be examined. Considering that the length of the data employed in this study (>100 beats on the average; Table I) was long enough to remove the respiration-induced variability in the BCG, the findings of this study (which primarily concerned the average BCG timings, time intervals, and amplitudes) may still be valid in both inspiratory and expiratory phases as long as the effect of the respiration on the BCG is consistent in both phases. But, this hypothesis could not be validated in this study due to

the limitation associated with the experimental data: reference respiratory measurement was not available. Future work must examine the effect of respiration-induced variability in the BCG on the relationship between the FP-BCG and WS-BCG, and more generally, on the relationship between the BCG obtained from diverse instruments.

V. CONCLUSIONS

The BCG is an attractive measurement means for CV health monitoring due to its close relationship to CV functions and its compatibility for a wide range of instrumentation modalities. However, this strength comes with a practical challenge in the universal analysis and interpretation of the BCG due to the heterogeneity of the BCG waveform morphology recorded with different instruments. This study intended to lay the foundation for the analysis and computational methods to enable standardized BCG signal analysis. The results illustrate that advanced signal processing may be effective in mitigating the instrument-induced variability in the morphology of the BCG waveform. Future work needs to invest efforts to more rigorously investigate computational methods for this purpose, as well as to apply such computational methods to enhance the efficacy of the BCG for CV health monitoring using a wide variety of instruments.

REFERENCES

- [1] I. Starr, "The Relation of the Ballistocardiogram to Cardiac Function," *Am. J. Cardiol.*, vol. 2, pp. 737–747, 1958.
- [2] M. B. Rappaport, "Displacement, Velocity, and Acceleration Ballistocardiograms as Registered with an Undamped Bed of Ultralow Natural Frequency III. The Normal Ballistocardiogram," Am. Heart J., vol. 52, no. 6, pp. 847–857, 1956.
- [3] O. Tannenbaum, J. A. Schack, and H. Vesell, "Relationship between Ballistocardiographic Forces and Certain Events in the Cardiac Cycle," *Circulation*, vol. VI, pp. 586–593, 1952.
- [4] A. Noordergraaf and C. E. Heynekamp, "Genesis of Displacement of the Human Longitudinal Ballistocardiogram from the Changing Blood Distribution," *Am. J. Cardiol.*, vol. 2, no. 6, pp. 748–756, 1958.
- [5] R. S. Gubner, M. Rodstein, and H. E. Ungerleider, "Ballistocardiography An Appraisal of Technic, Physiologic Principles, and Clinical Value," *Circulation*, vol. VII, pp. 268–287, 1953.
- [6] W. R. Scarborough, R. E. Mason, F. W. Davis, M. L. Singewald, B. M. Baker, and S. A. Lore, "A ballistocardiographic and Electrocardiographic Study of 328 Patients with Coronary Artery Disease: Comparison with Results from a Similar Study of Apparently Normal Persons," Am. Heart J., vol. 44, no. 5, pp. 645–670, 1952.
- [7] L. M. Bargeron, "The Force Ballistocardiogram as an Index of Severity in Congenital Aortic Stenosis," *Circulation*, vol. 37, pp. 238–243, 1968.
- [8] W. R. Scarborough, "Current Status of Ballistocardiography," Prog. Cardiovasc. Dis., vol. 2, no. 3, pp. 263–291, 1959.
- [9] D. W. Jung, S. H. Hwang, H. N. Yoon, Y. G. Lee, D. Jeong, and K. S. Park, "Nocturnal Awakening and Sleep Efficiency Estimation Using Unobtrusively Measured Ballistocardiogram," *IEEE Trans. Biomed. Eng.*, vol. 61, no. 1, pp. 131–138, 2014.
- [10] J. H. Shin, Y. J. Chee, D. Jeong, and K. S. Park, "Nonconstrained Sleep Monitoring System and Algorithms Using Air-Mattress With Balancing Tube Method," *IEEE J. Biomed. Heal. Informatics*, vol. 14, no. 1, pp. 147–156, 2010.
- [11] E. Pinheiro, O. Postolache, and P. Girão, "Non-Intrusive Device for Real-Time Circulatory System Assessment with Advanced Signal Processing Capabilities," *Meas. Sci. Rev.*, vol. 10, no. 5, pp. 166–175, 2010.
- [12] A. Akhbardeh, S. Junnila, T. Koivistoinen, and A. Varri, "An

- intelligent Ballistocardiographic Chair using a Novel SF-ART Neural Network and Biorthogonal Wavelets," *J. Med. Syst.*, vol. 31, no. 1, pp. 69–77, 2007.
- [13] O. T. Inan, M. Etemadi, R. M. Wiard, L. Giovangrandi, and G. T. A. Kovacs, "Robust Ballistocardiogram Acquisition for Home Monitoring," *Physiol. Meas.*, vol. 30, pp. 169–185, 2009.
- [14] O. T. Inan, D. Park, S. Member, L. Giovangrandi, and G. T. A. Kovacs, "Noninvasive Measurement of Physiological Signals on a Modified Home Bathroom Scale," *IEEE Trans. Biomed. Eng.*, vol. 59, no. 8, pp. 2137–2143, 2012.
- [15] J. H. Shin, K. M. Lee, and K. S. Park, "Non-Constrained Monitoring of Systolic Blood Pressure on a Weighing Scale," *Physiol. Meas.*, vol. 30, pp. 679–693, 2009.
- [16] D. Da He, E. S. Winokur, and C. G. Sodini, "An Ear-Worn Vital Signs Monitor," *IEEE Trans. Biomed. Eng.*, vol. 62, no. 11, pp. 2547– 2552, 2015.
- [17] C.-S. Kim, A. M. Carek, R. Mukkamala, O. T. Inan, and J.-O. Hahn, "Ballistocardiogram as Proximal Timing Reference for Pulse Transit Time Measurement: Potential for Cuffless Blood Pressure Monitoring," *IEEE Trans. Biomed. Eng.*, vol. 62, no. 11, pp. 2657– 2664, 2015.
- [18] S. L. Martin et al., "Weighing Scale-Based Pulse Transit Time is a Superior Marker of Blood Pressure than Conventional Pulse Arrival Time," Sci. Rep., vol. 6, no. November, p. 39273, 2016.
- [19] C.-S. Kim, A. M. Carek, O. T. Inan, R. Mukkamala, and J.-O. Hahn, "Ballistocardiogram-Based Approach to Cuffless Blood Pressure Monitoring: Proof of Concept and Potential Challenges," *IEEE Trans. Biomed. Eng.*, vol. 65, no. 11, pp. 2384–2391, 2018.
- [20] D. Campo *et al.*, "Measurement of Aortic Pulse Wave Velocity With a Connected Bathroom Scale," *Am. J. Hypertens.*, pp. 1–8, 2017.
- [21] M. Etemadi, S. Member, O. T. Inan, L. Giovangrandi, and G. T. A. Kovacs, "Rapid Assessment of Cardiac Contractility on a Home Bathroom Scale," *IEEE Trans. Biomed. Eng.*, vol. 15, no. 6, pp. 864–869, 2011.
- [22] H. Ashouri, L. Orlandic, and O. T. Inan, "Unobtrusive Estimation of Cardiac Contractility and Stroke Volume Changes using Ballistocardiogram Measurements on a High Bandwidth Force Plate," Sensors (Switzerland), vol. 16, no. 6, p. 787, 2016.
- [23] A. D. Wiens, M. Etemadi, S. Roy, L. Klein, and O. T. Inan, "Toward Continuous, Noninvasive Assessment of Ventricular Function and Hemodynamics: Wearable Ballistocardiography," *IEEE J. Biomed. Heal. Informatics*, vol. 19, no. 4, pp. 1435–1442, 2015.
- [24] C.-S. Kim et al., "Ballistocardiogram: Mechanism and Potential for Unobtrusive Cardiovascular Health Monitoring," Sci. Rep., vol. 6, p. 31297, 2016
- [25] S. A. Talbot and W. K. Harrison, "Dynamic Comparison of Current Ballistocardiographic Methods Part II: Effect of a Platform in Ballistocardiographic Dynamics," *Circulation*, vol. 12, no. 5, pp. 845–857, 1955.
- [26] R. P. Walker, T. J. Reeves, K. Willis, L. Christianson, J. R. Pierce, and D. Kahn, "The Effect of Surface and Recording Technique on the Direct Ballistocardiogram," Am. Heart J., vol. 46, no. 2, pp. 166–179, 1953.
- [27] H. C. Burger, A. Noordergraaf, J. J. M. Korsten, and P. Ullersma, "Physical Basis of Ballistocardiography. IV The Relative Movement of Subject and Ballistocardiogram," *Am. Heart J.*, vol. 52, no. 2, pp. 653–673, 1956.
- [28] D. P. Garg and M. a. Ross, "Vertical Mode Human Body Vibration Transmissibility," *IEEE Trans. Syst. Man. Cybern.*, vol. SMC-6, no. 2, pp. 102–112, 1976.
- [29] M. J. Griffin and Y. Matsumoto, "Dynamic Response of the Standing Human Body Exposed To Vertical Vibration: Influence of Posture and Vibration Magnitude," J. Sound Vib., vol. 212, no. 1, pp. 85–107, 1998.
- [30] K. J. Keesman, System Identification-An Introduction. London: Springer-Verlag, 2011.

DISCLOSURE

O. T. Inan is a Scientific Advisor to, and has patents licensed by, Physiowave, Inc., a manufacturer of BCG measurement hardware.